H-atom Positional Corrections, Spin Splitting, and Thermodynamic Equilibria in Hybrid Organic-Inorganic Perovskites

Gabriel J. Graf[1], Yi Xie[1], Grace Dono[1,2], Gabrielle Koknat[1], Vania Chopra[1], Rayan Chakraborty[1], Purusharth Amrut[1],, Nicholas J. Weadock[3],
Xiaoping Wang[4], Ruyi Song[1], Michael Toney[3], David Mitzi[1], Volker Blum[1]

1. Duke University, Thomas Lord Department of Mechanical Engineering and Materials Science, Durham, NC. 2. University of Rochester, Department of Physics and Astronomy, Rochester, NY.
3. Department of Chemical and Biological Engineering, University of Colorado, Boulder, Boulder, Colorado. 4. Neutron Scattering Division, Oak Ridge National Laboratory, Oak Ridge, Tennessee

Abstract

Hybrid Organic-Inorganic Perovskites (HOIPs) are semiconducting materials with significant potential in optoelectronic and spintronic devices. X-ray diffraction (XRD) provides a cost-effective method for determining atomic positions in HOIPs but struggles to accurately locate low-electron-density atoms like hydrogen. To address this, a technique developed within the group applies hydrogen-specific density functional theory (DFT) relaxation to correct hydrogen atomic positions, achieving good agreement with advanced methods like neutron scattering. This work extends the approach to the HybriD^3 database by performing extensive "H-relaxation" of XRD structures to provide more geometrically accurate configurations. The spin-splitting magnitudes in four methylbenzylammonium lead iodide-based HOIPs were calculated using FHI-aims. For the $(CF_3\text{-MBA})_2PbI_4$ system, which exhibits site disorder, a configurational selection method combining MACE force field and all-atom DFT relaxation was used to establish the most thermodynamically stable configuration. Using DFT, the hydrogen atom positions in these structures were relaxed and band structures were calculated using the PBE-TS and HSE06-TS functional-dispersion correction pairs, respectively. Finally, phase equilibrium studies provide insights into the ideal HOIP synthesis, degradation, and operating conditions. Prior work on the 3D HOIP $MAPbI_3$ is discussed and initial work on the study of thermodynamic equilibrium in 2D phenethylammonium lead iodide (PEPI) is presented.

Correction of XRD Structures

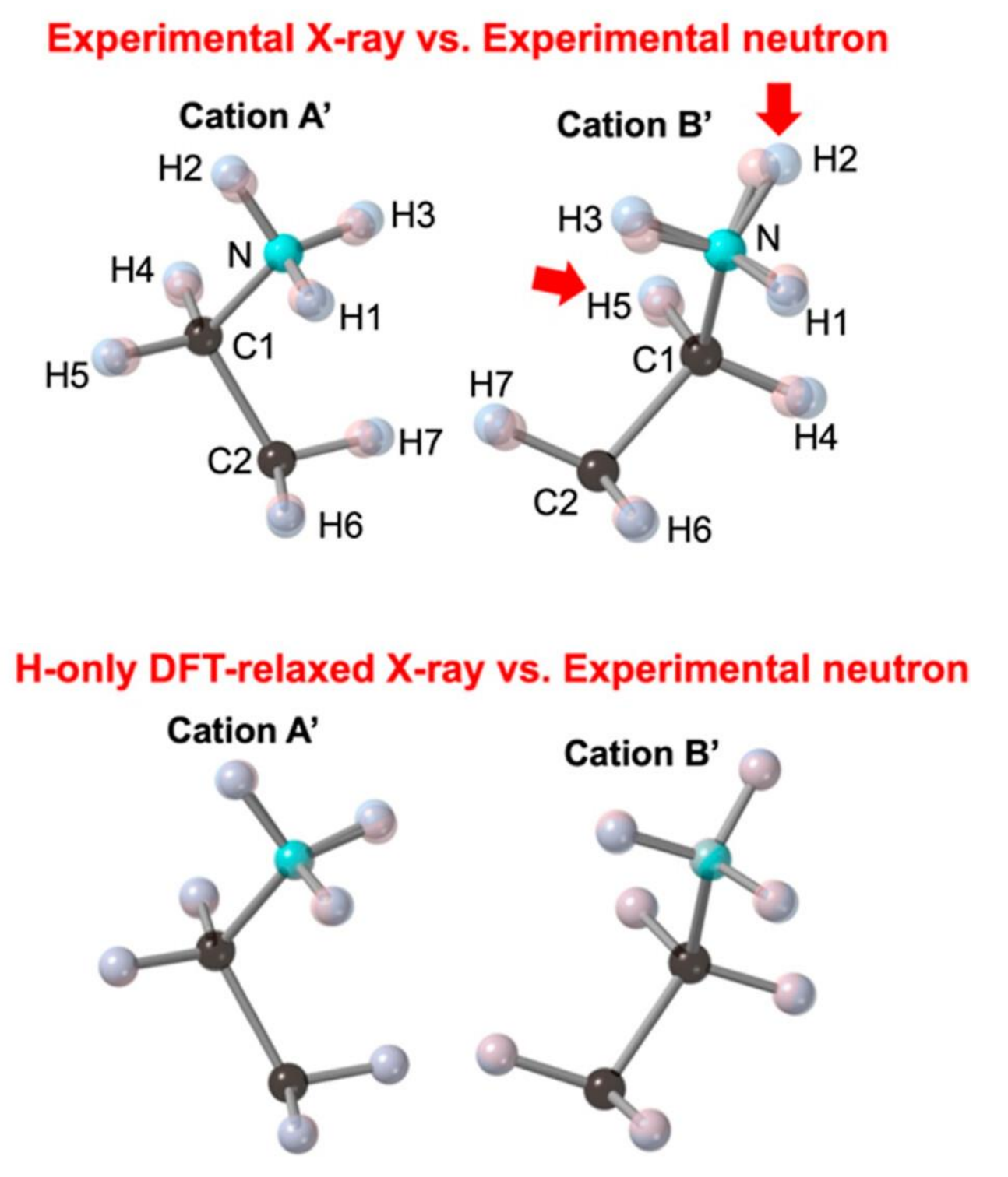

Above: Comparison of hydrogen bond lengths in experimental X-ray structures before and after hydrogen-only DFT relaxation, with reference to neutron scattering structures. X-ray diffraction (XRD) measurements significantly underestimate C-H and N-H bond lengths when compared to neutron scattering structures. Hydrogen-only DFT relaxation yields bond lengths that closely align with those determined by neutron scattering. Adapted from Xie *et al.* 2024.

Below: Demonstration of the systematic inaccuracy in hydrogen positions on the ethylammonium group in the $(2\text{-BrPEA})_2PbI_4$ system determined by X-ray diffraction compared to neutron scattering. Density functional theory can correct the locations of the X-ray structure to good agreement with structures from neutron scattering. Figure adapted from Xie *et al.* 2024.

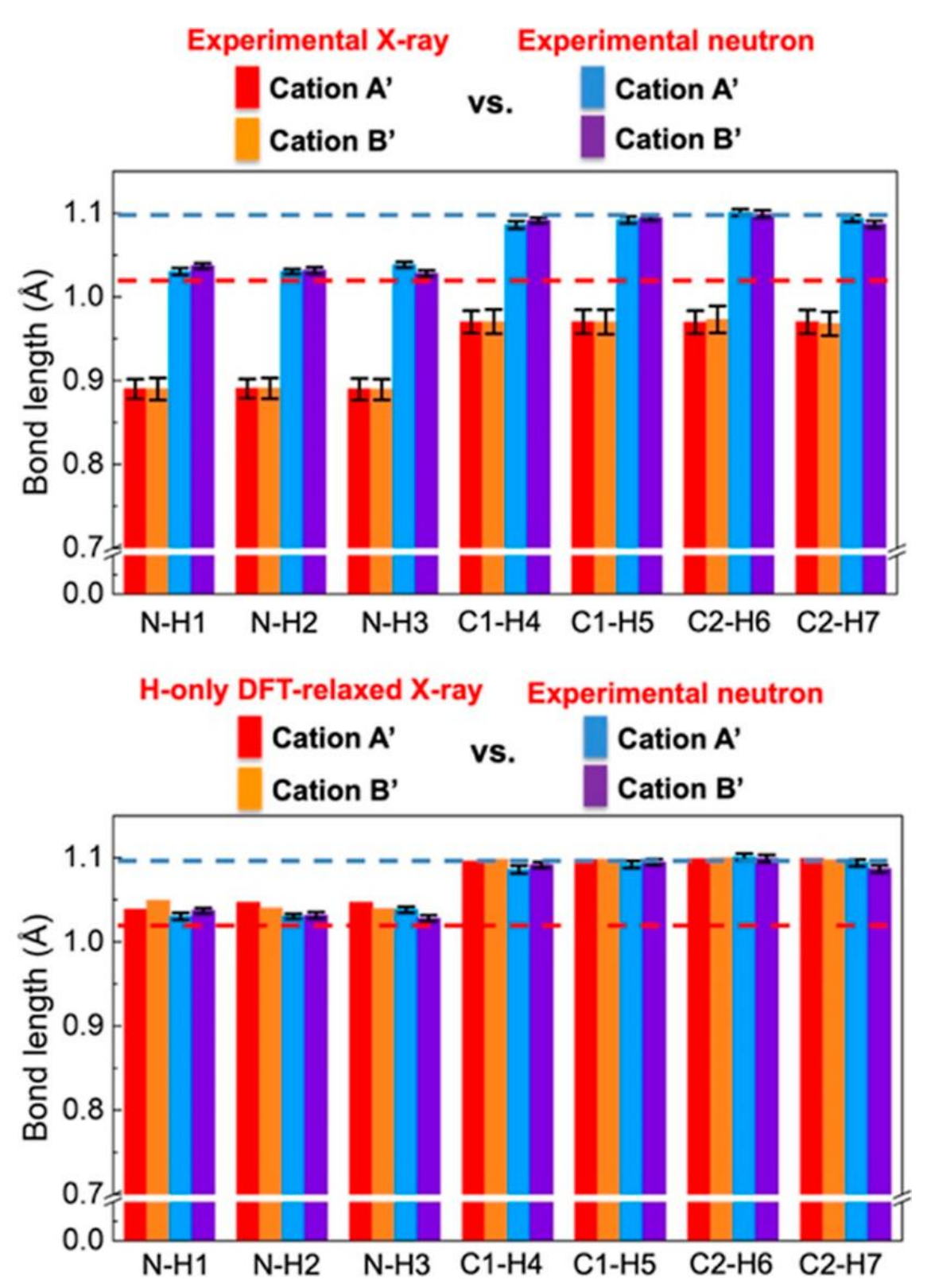

	80 K H-only DFT-relaxed X-ray vs experimental X-ray	80 K/90 K H-only DFT-relaxed X-ray vs experimental neutron
total energy difference	43.756 eV	0.357 eV
max H position difference	0.207 Å	0.084 Å
max N-H bond length difference	0.147 Å (16.46%)	0.019 Å (1.83%)
max C-H bond length difference	0.131 Å (13.49%)	0.014 Å (1.26%)

Left: A table summarizing the energetic and hydrogen positional changes in the experimental X-ray structure of $(2\text{-PEA})_2PbI_4$ after hydrogen-only relaxation using DFT. The hydrogen-relaxed XRD structure shows a substantial total energy difference from the experimental XRD structure but minimal differences relative to the neutron scattering structure. Furthermore, the hydrogen positions and bond lengths in the hydrogen-relaxed XRD structure closely resemble those in the neutron scattering structure. Adapted from Xie et al., 2024.

Below: A table showing the difference of hydrogen atom positions in six experimental XRD structure datasets from the HybriD^3 database after hydrogen-only DFT relaxation. The final structures were relaxed using the PBE-TS level of theory and "tight" numerical accuracy settings in FHI-aims. Experimental XRD data for each system was taken from the dataset in the HybriD^3 database with the listed dataset ID. * indicates this compound was only "hydrogen-relaxed" up to intermediate settings due to SCF convergence issues.

IUPAC Name	Dataset ID	C-H Hydrogen Position Difference (Å)	N-H Hydrogen Position Difference (Å)
5,5‘‘‘-bis(aminoethyl)-2,2‘:5‘,2‘‘:5‘‘,2‘‘‘-quaterthiophene lead(II) bromide*	217	0.0677 ± 0.0237	0.1794 ± 0.1010
4-fluorophenethanaminium lead (II) iodide	2008	0.1485 ± 0.0125	0.2045 ± 0.0152
3-(N,N-dimethanaminium)-propane-1-aminium lead (II) bromide	536	0.1384 ± 0.0045	0.1360 ± 0.0357
benzene-1,4-di(methanaminium) lead (II) iodide	2010	0.1386 ± 0.0101	0.1184 ± 0.0330
benzene-1,4-di(methanaminium) lead (II) bromide	2011	0.1395 ± 0.0102	0.1244 ± 0.0380
1-methyl-1-butanaminium lead (II) iodide	564	0.1644 ± 0.0243	0.1674 ± 0.0066

Xie, Y.; Koknat, G.; Weadock, N. J.; Wang, X.; Song, R.; Toney, M. F.; Blum, V.; Mitzi, D. B. Hydrogen Bonding Analysis of Structural Transition-Induced Symmetry Breaking and Spin Splitting in a Hybrid Perovskite Employing a Synergistic Diffraction-DFT Approach. Journal of the American Chemical Society 2024, 146 (32), 22509–22521. https://doi.org/10.1021/jacs.4c06287.

Spin Splitting in 2D Hybrid Perovskites

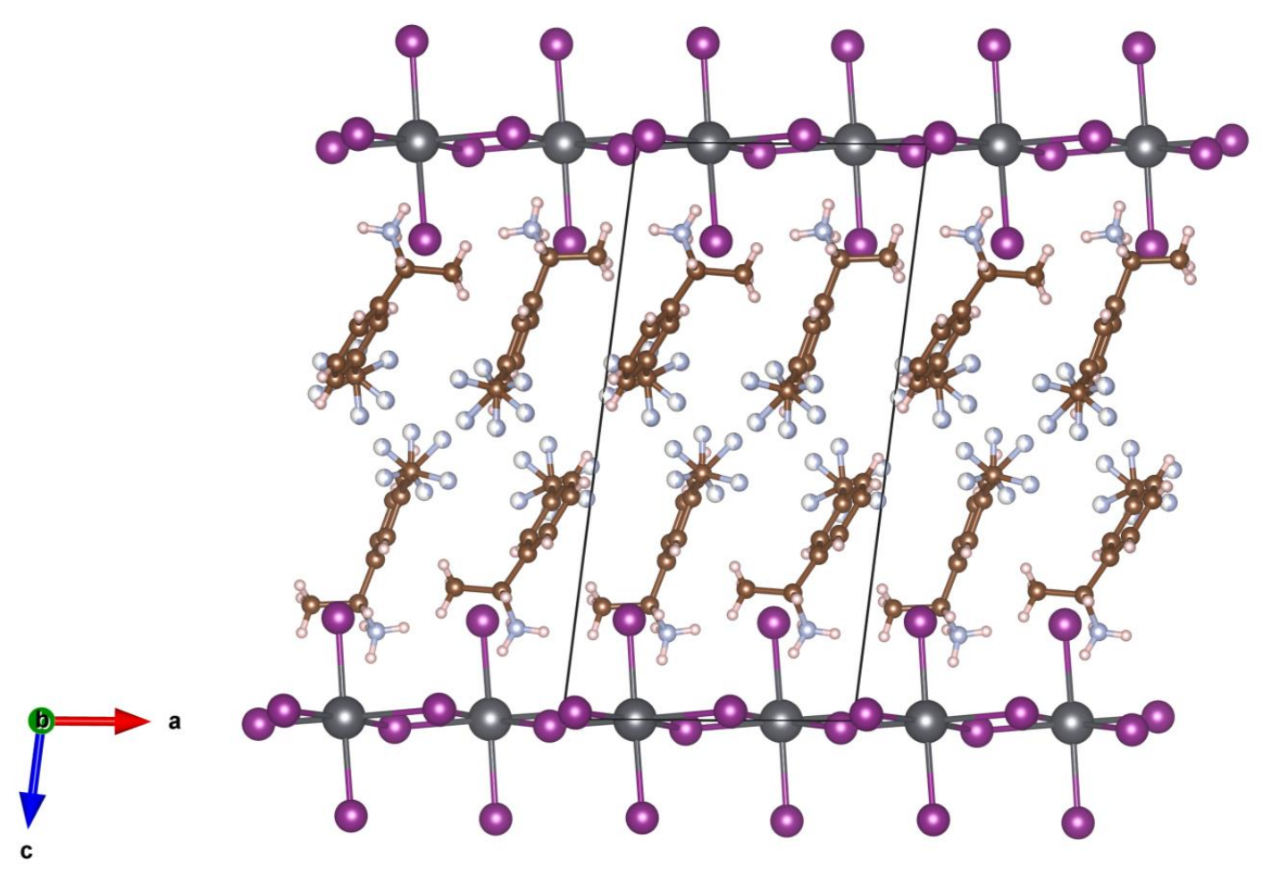

Experimental XRD crystal structure of $(R\text{-}3\text{-}CF_3MBA)_2PbI_4$. The crystal structure shows the significant site disorder of the fluorine positions on the $-CF_3$ substituent. Octahedral tilting can also be observed.

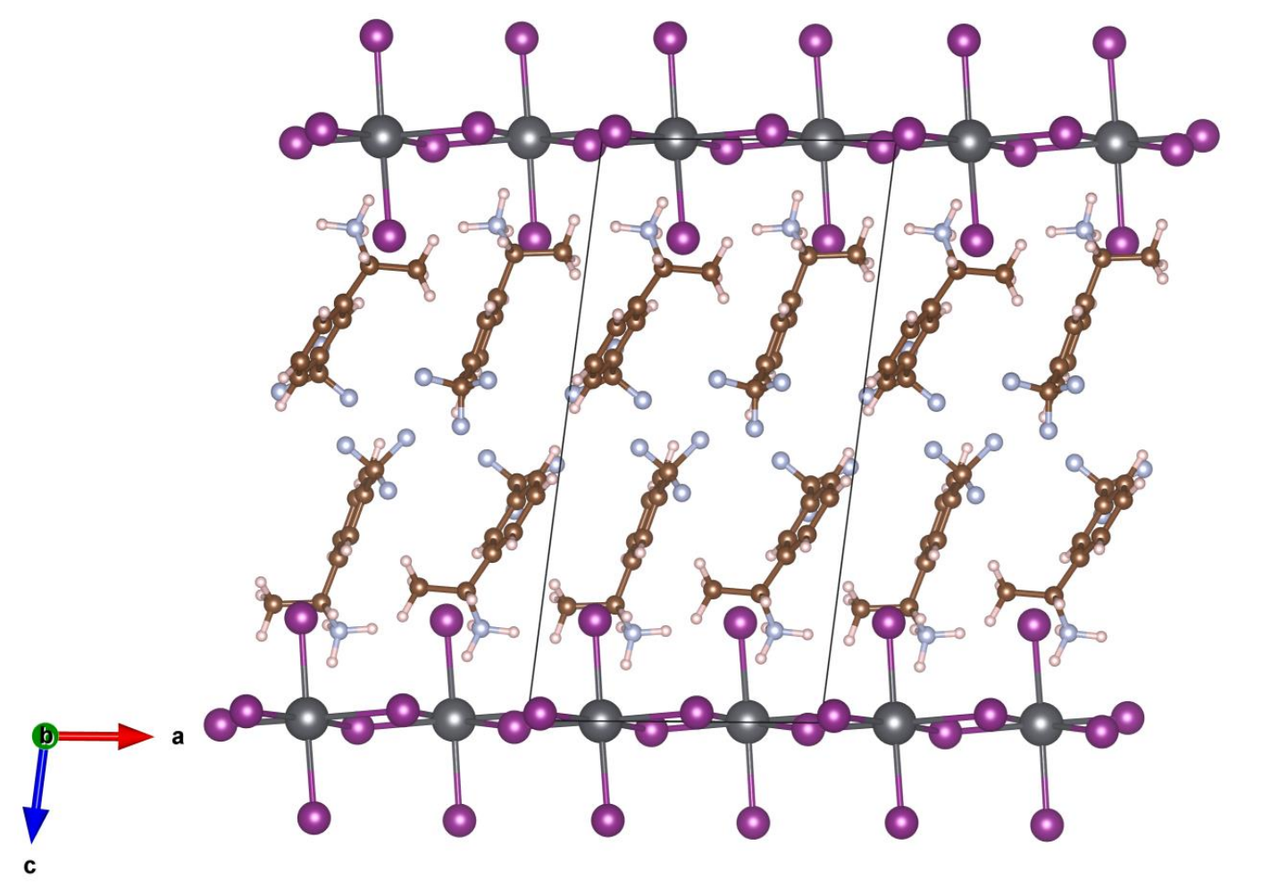

Crystal structure after determination of most thermodynamically stable configuration and hydrogen atom relaxation.

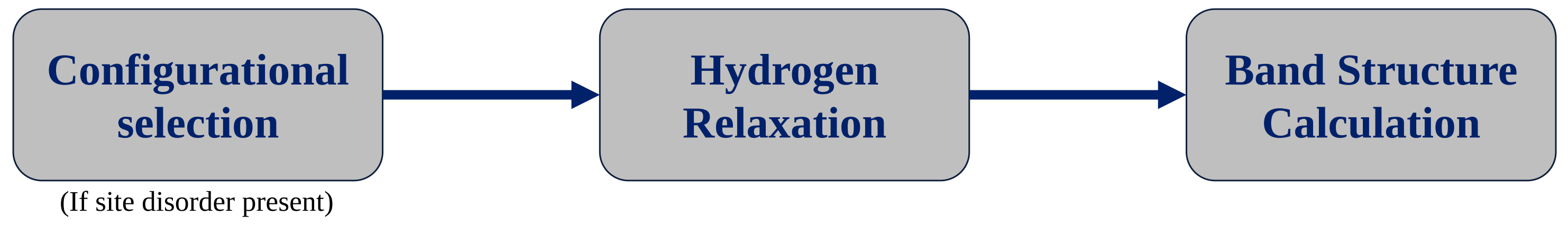

Configurational selection → **Hydrogen Relaxation** → **Band Structure Calculation**

(If site disorder present)

Above: The computational workflow for 2D perovskite spin splitting analysis from experimental XRD structure. Configurational selection begins with the .cif file of a 2D hybrid perovskite obtained by XRD. If site disorder is present, each possible configuration is relaxed to energy minimum using a MACE force field relaxation followed by an all-atom DFT geometry optimization using "light" settings in FHI-aims. The positions of the hydrogen atoms in the .cif file corresponding to the most stable structure are then relaxed using the PBE-TS functional-dispersion correction pair with "tight" numerical accuracy settings in FHI-aims. Finally, the band structure is calculated using the HSE06-TS hybrid functional with "tight" numerical accuracy settings. The spin splitting from the data is shown below. An additional note is that doing a MACE force field relaxation followed by a "light" DFT relaxation yielded a different lowest energy compound from doing "light" DFT relaxations only for every compound, this inconsistency is currently being investigated. The $(R\text{-}3\text{-}CF_3MBA)_2PbI_4$ data (denoted by *) is therefore still preliminary.

Right: Schematic representation of the Rashba-Dresselhaus spin splitting magnitude, ΔE. E^+ and E^- are the bands corresponding to the positive and negative spin states. k_0 is the momentum shift of the conduction band minimum. E_{RD} energetic difference between the conduction band minimum and the Γ point.

Far right: The Brillouin zone corresponding to the band structures below. The a-b plane corresponds to the in-plane direction of the 2D hybrid perovskites in real space.

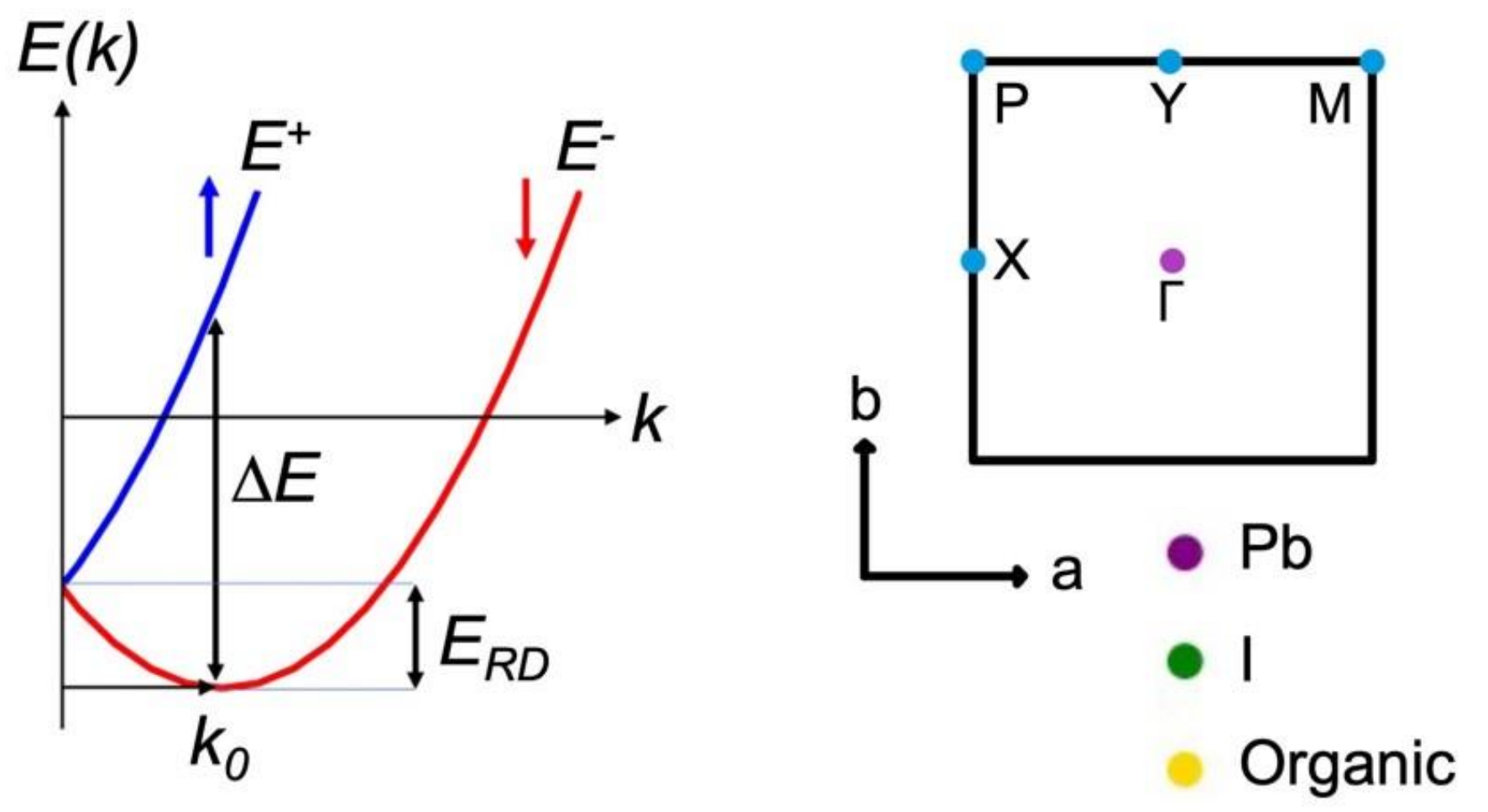

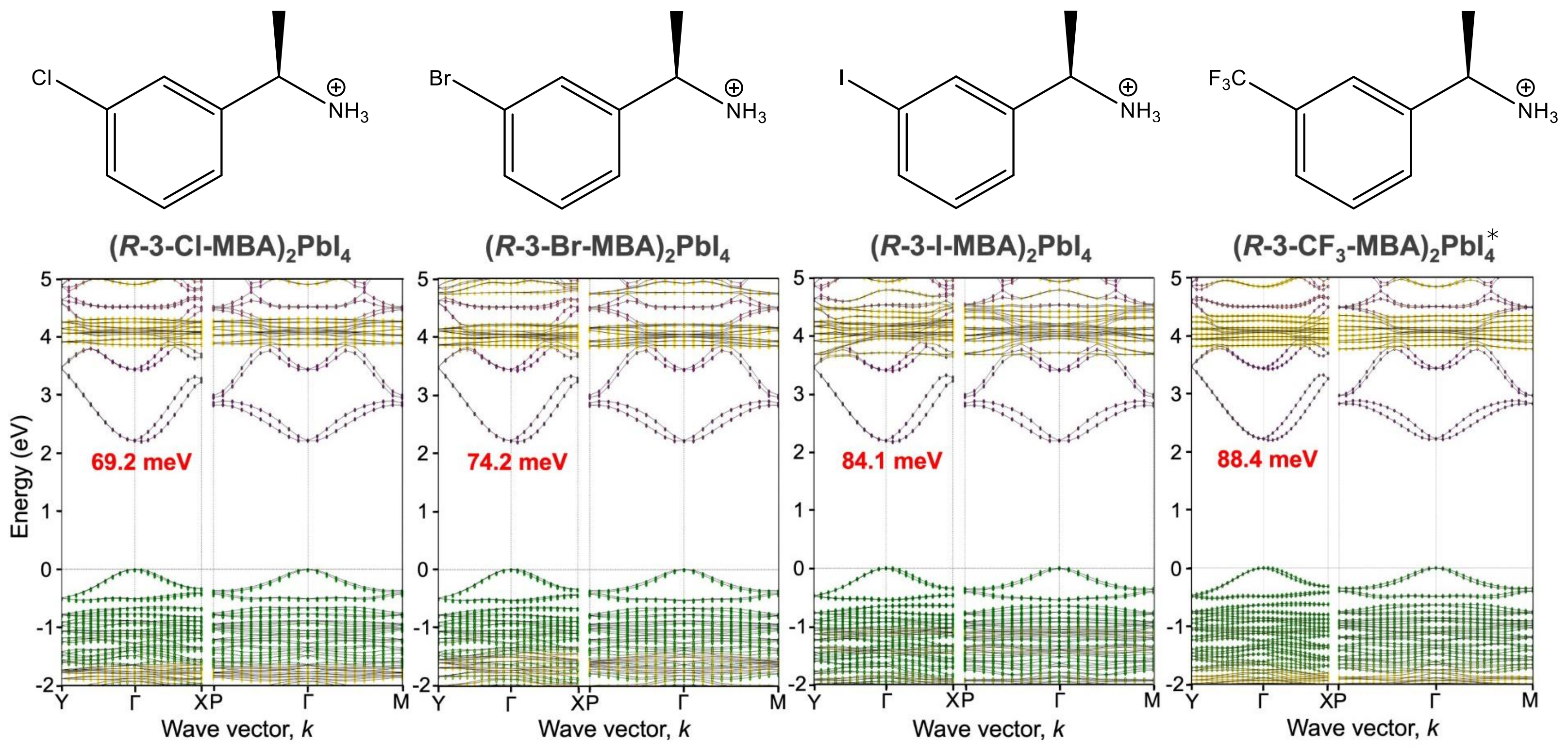

Above: The band structures of four 2D lead iodide-based hybrid organic-inorganic perovskites. The structures of the organic component in each of the hybrid perovskites are shown above the diagrams. The band structures are calculated at the HSE06-TS level of theory with exchange mixing of 0.25 and a screening parameter of 0.11 inverse Bohr radii.

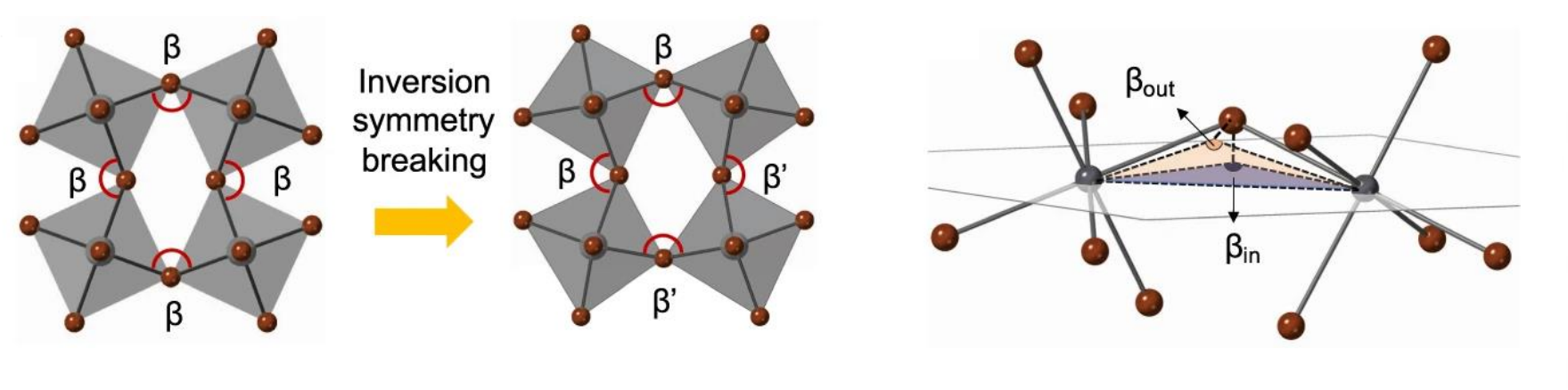

Above: Figure from Jana *et al.* 2021 which demonstrates in-plane and out-of-plane inversion symmetry breaking in a 2D perovskite material.

Right: The agreement between $\Delta\beta_{in}$ and the calculated spin splitting magnitude. $\Delta\beta_{in}$ is quantified from the experimentally determined crystal structure, and spin splitting magnitude is determined from the band structure calculated by DFT.

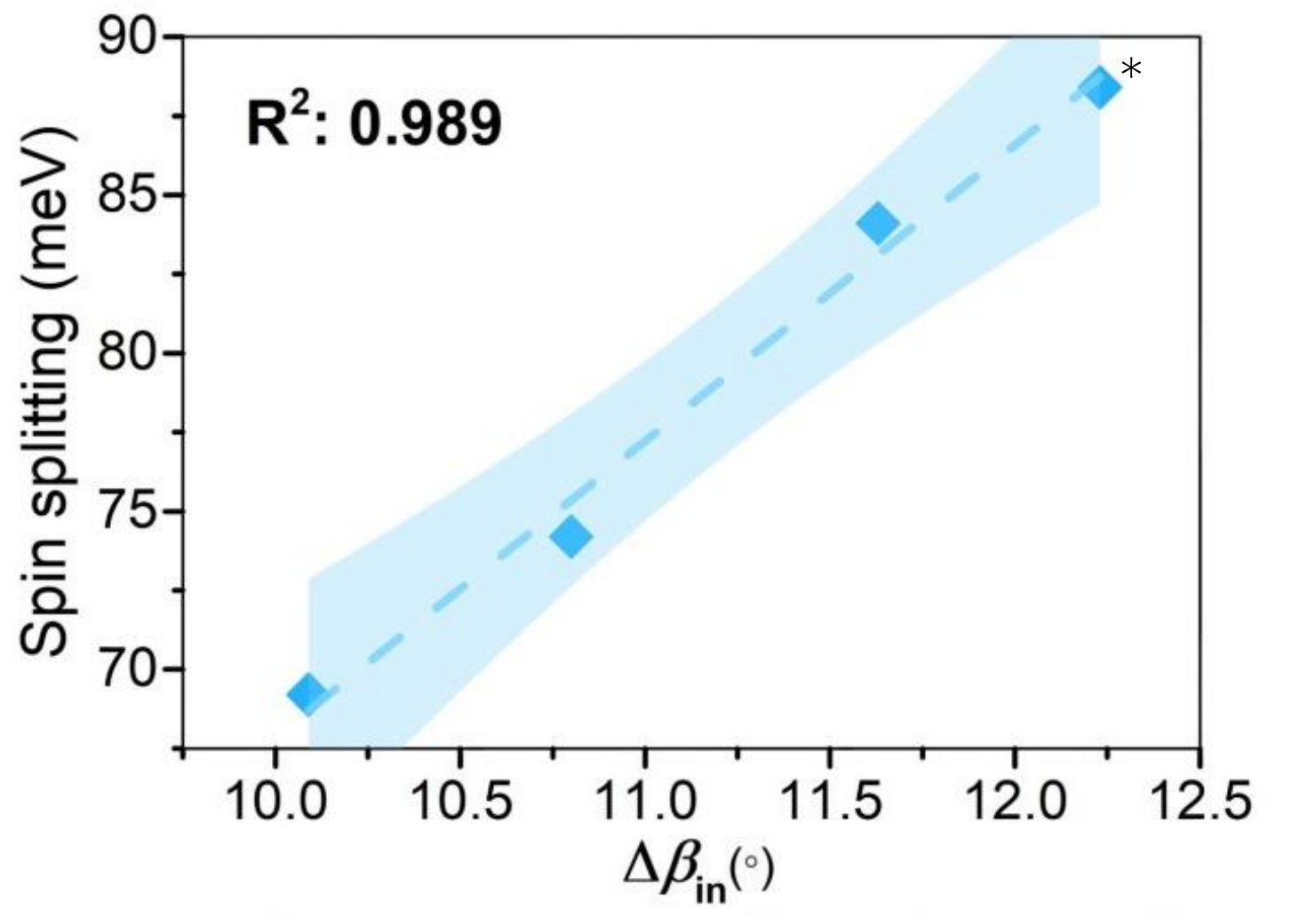

Jana, M. K.; Song, R.; Xie, Y.; Zhao, R.; Sercel, P. C.; Blum, V.; Mitzi, D. B. Structural Descriptor for Enhanced Spin-Splitting in 2D Hybrid Perovskites. Nature Communications 2021, 12 (1). https://doi.org/10.1038/s41467-021-25149-7.

Brillouin zone map, spin splitting schematic, band structures, and the figure showing spin splitting correlation with $\Delta\beta_{in}$ are from a manuscript in process. Xie *et al.*

Thermodynamic Equilibria

Background Information

$$(CH_3NH_3)PbI_3\,(s) \rightarrow PbI_2(s) + CH_2NH_2(g) + HI\,(g)$$

Right: The equation for change in free energy used to calculate thermodynamic equilibrium conditions. Δg is the total change in free energy, e_0 is the internal energy for a given species, and Δs_{mix} is the mixing entropy. For the solid species, f(T) corresponds to the vibrational free energy. For the gaseous species, f_{rv} and f_{trans} correspond to the rovibrational and translational free energies, respectively.

$$\Delta g = e_{0,\mathrm{PbI2}} + f_{\mathrm{PbI2}}(T) + e_{0,\mathrm{HI}} + f_{\mathrm{trans,HI}}(T,p) + f_{rv,\mathrm{HI}}(T) + e_{0,\mathrm{MAe}} + f_{\mathrm{trans,MAe}}(T,p) + f_{rv,\mathrm{MAe}}(T) - T\cdot\Delta s_{\mathrm{mix}} - e_{0,\mathrm{MAPbI3}} - f_{\mathrm{MAPbI3}}(T).$$

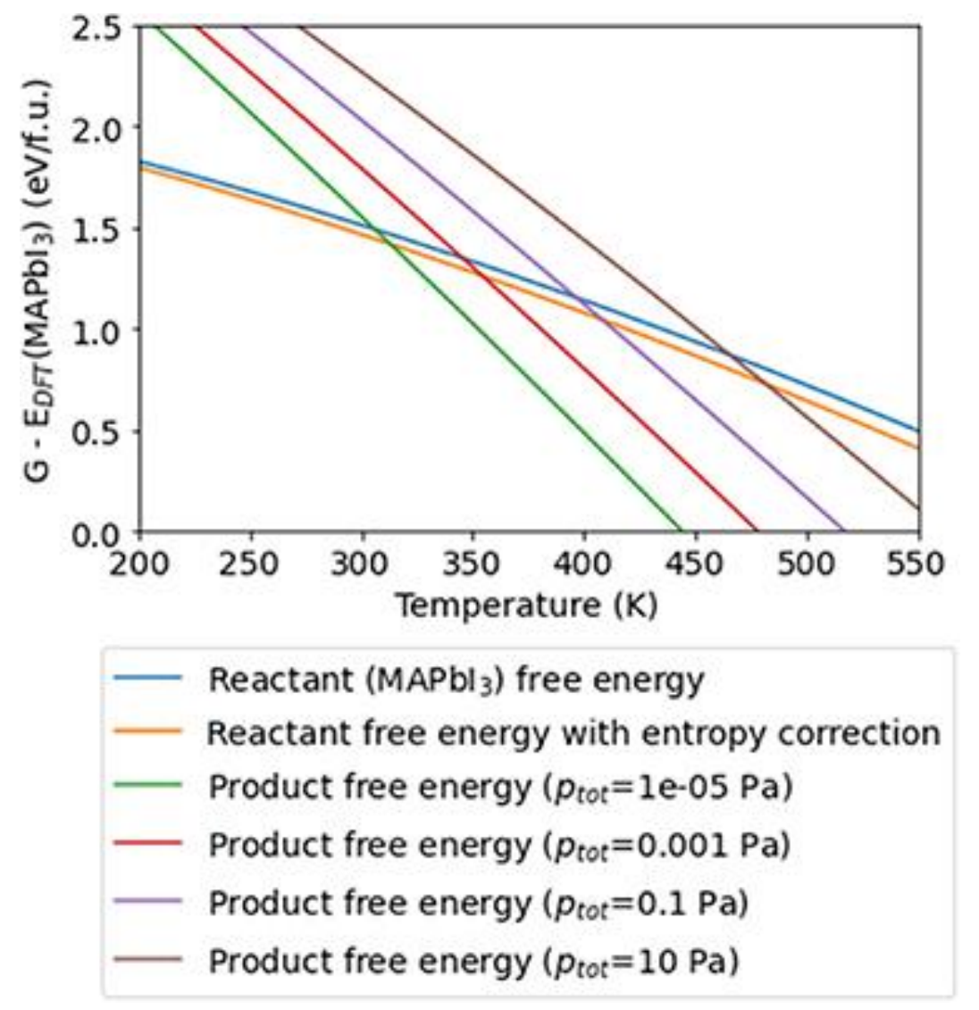

Above: The Gibbs free energy of $MAPbI_3$ as a function of temperature, with and without the configurational entropy correction. The Gibbs free energies of the products as a function of temperature are shown at four selected pressures. Adapted from Heine *et al.* 2024.

Method	Reaction internal energy change (eV / formula unit)
PBE + TS	2.403
HSE06 + TS	2.487
PBE0 + TS	2.465

Above: The total change in internal energy of the decomposition reaction for each formula unit of $MaPbI_3$, as calculated at three levels of theory. The positive values indicate that the $MAPbI_3$ is stable against decomposition before rotational, vibrational, and translational corrections are applied. Adapted from Heine *et al.* 2024.

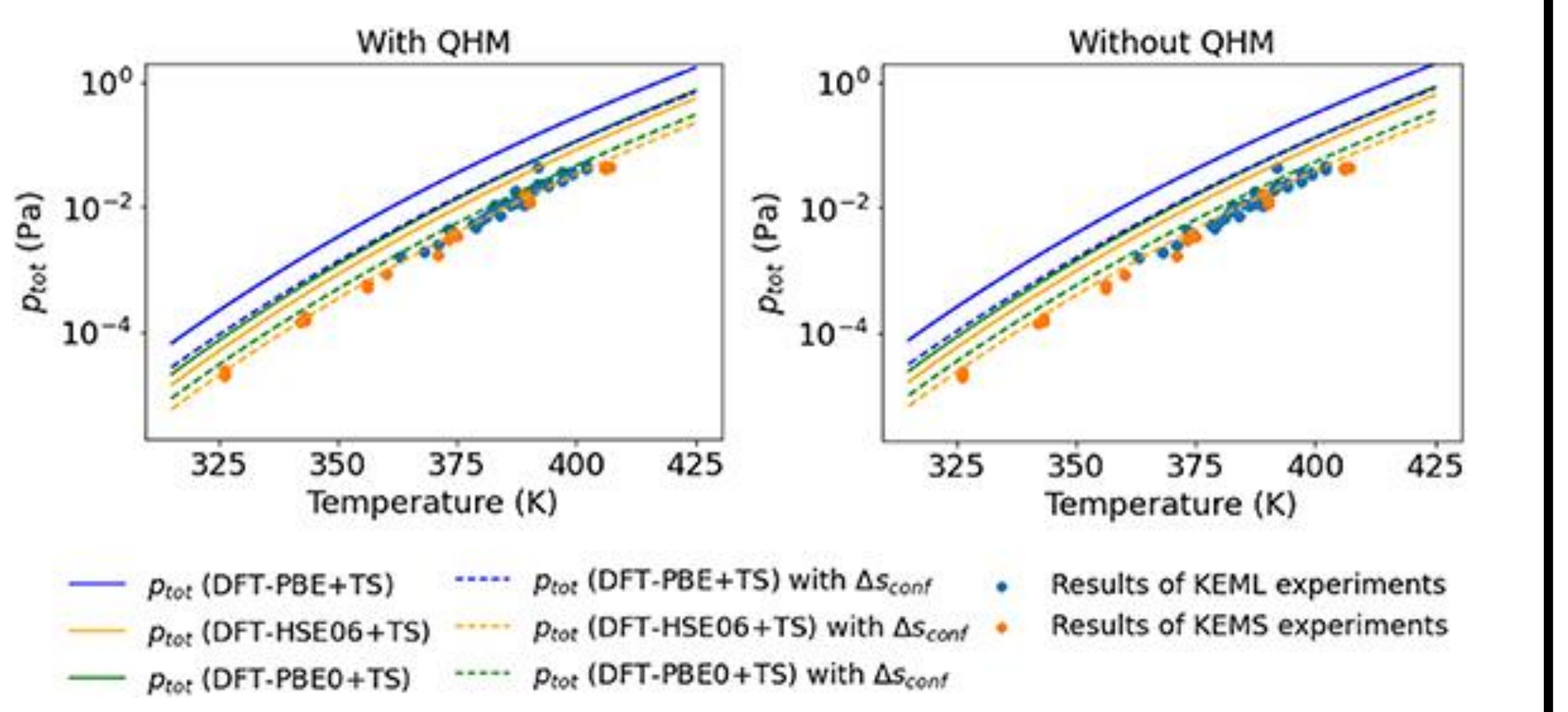

Above: A comparison of temperature-pressure equilibria calculated with and without the quasi-harmonic approximation (QHM) using density functional theory (DFT) in FHI-aims with experimental data from KEML and KEMS studies reported by Brunetti et al. (2016). Each participating species was relaxed with the functional listed above, and vibrational and entropy terms were subsequently computed using the PBE-TS functional. A configurational entropy correction, $\Delta S_{conf} = k_B \ln(6)$, was applied to account for the six possible orientations of the MA cation in the 3D perovskite structure. Adapted from Heine *et al.* 2024.

Species	Zero-point energy (eV / formula unit)
MA	1.689
HI	0.141
PbI_2	0.037
$MAPbI_3$	2.146
Reaction energy change	-0.279

Above: The zero-point energies of the participating species, as calculated at the PBE-TS level of theory. The total reaction energy change after zero point energy calculation lowers the energy gap between the products and the reactants, corresponding to lower stability of $MAPbI_3$ against degradation. Adapted from Heine *et al.* 2024.

Current Focus

$$(PEA)_2PbI_4\,(s) \rightarrow PbI_2(s) + 2\,PEA\,(g) + 2\,HI\,(g)$$

Brunetti, B.; Cavallo, C.; Ciccioli, A.; Gigli, G.; Latini, A. On the Thermal and Thermodynamic (In)Stability of Methylammonium Lead Halide Perovskites. Scientific Reports 2016, 6 (1). https://doi.org/10.1038/srep31896.
Heine, D.; Yu, H.-C.; Blum, V. Benchmark Thermodynamic Analysis of Methylammonium Lead Iodide Decomposition from First Principles. Journal of Physics Energy 2023, 6 (1), 015015–015015. https://doi.org/10.1088/2515-7655/ad139d.

Future Work

- ☐ Construct a full equilibrium phase diagram to study the degradation of $(PEA)_2PbI_4$ as well as other hybrid perovskite systems
- ☐ Design methods to predict solid-solid phase transitions in hybrid perovskites as a function of chemical potential and quantify their effects on electronic properties
- ☐ Calculate the spin-splitting magnitudes and spin textures of more 2D hybrid perovskites and further investigate the relationship between $\Delta\beta_{in}$ and the spin-splitting magnitude.
- ☐ Develop a method to accurately predict the most thermodynamically stable configuration of a site-disorder 2D hybrid perovskites that is more computationally affordable when multiple possible combinations are present.
- ☐ Expand the hydrogen relaxation of experimental X-ray structures to other systems in the HybriD^3 database.

Contributions and Acknowledgements

The corrections of hydrogen positions in XRD-determined HOIP structures were completed by Vania Chopra as an undergraduate independent study under the supervision and guidance of Gabriel Graf and Professor Volker Blum. Neutron scattering data was collected by Dr. Yi Xie, Dr. Nicolas Weadock, Professor Michael Toney, and Dr. Xiaoping Wang. The configurational selections, hydrogen relaxations, and band structure calculations for the 2D HOIP spin-splitting study were completed by Gabriel Graf and Grace Dono, with assistance from Dr. Rayan Chakraborty. XRD crystal structures were provided by Dr. Yi Xie from the lab group of Professor David Mitzi. Yi and Gabriel also created the figures for the spin-splitting study. Additional experimental work on $(R\text{-}3\text{-}CF_3\text{-}MBA)_2PbI_4$ was conducted by Purusharth Amrut. Previous research on the $MAPbI_3$ decomposition was conducted by Douglas Heine under the supervision of Professor Volker Blum. Preliminary research on a similar decomposition pathway for $(PEA)_2PbI_4$ was conducted by Gabriel Graf.